P16

PREPARATION AND STRUCTURE OF TiO_2 NANOTUBES

E. Pavlová[1], M. Lapčíková[1], M. Šlouf[1,2], R. Kužel[3]

[1]Institute of Macromolecular Chemistry, Academy of Sciences of the Czech Republic, Heyrovskeho nam. 2, 162 06 Praha 6, Czech Republic
[2]Member of Consortium for Research of Nanostructured and Crosslinked Polymeric Materials (CRNCPM)
[3]Department of Electronic Structures, Faculty of Mathematics and Physics, Charles University, 121 16 Praha 2, Ke Karlovu 5, Czech Republic, slouf@imc.cas.cz

Titanium oxide nanotubes were synthetized and characterized by means of high-resolution scanning electron microscopy (SEM, STEM, EDS) and powder X-ray diffraction (PXRD). The prepared TiO_2 nanotubes represent quite new morphology of TiO_2 (cf. Figs. 1 and 2). Their crystalline structure is different from all common modifications of TiO_2, i.e. rutile, anatase and brookite (Fig. 3).

Synthesis of the TiO_2 nanotubes was based on the procedures described elsewhere [1, 2]. Titanium oxide powder (from Aldrich; Fig. 1) in 10 M aqueous NaOH solution was placed in a 250 ml teflon flask, which, in turn, was placed for 24 h in an oil bath at 120 °C. The mixture was washed with distilled water till the pH of solution was approx. 8. The product was left in the form of water suspension, where it is stable for at least several months. We managed to sytnthetize TiO_2 nanotubes not only from pure anatase as stated in ref. [3], but also from the mixture of modifications, anatase and rutile using TiO_2 nanopowder or TiO_2 technical powder (both supplied by Aldrich). The first series of the specimens (denotes as: specimens from solution) for SEM and PXRD was prepared as follows: the TiO_2 nanotubes in water suspension were dispersed by means of ultrasonication and then a small drop was put to the microscopic support glass and left to evaporate (Fig. 2). The second series of the specimens (specimens from powder) was prepared by filtration of the TiO_2 nanotubes and the filtrate was dried completely at room temperature. However, SEM observations showed that the second preparation procedure leads to partial merging of the single TiO_2 nanotubes into agglomerates.

Powder patterns of TiO_2 technical powder (P01), TiO_2 nanopowder (P02), TiO_2 nanotubes from the first preparation procedure (G01) and TiO_2 nanotubes from the second procedure described above (P03) are shown in Fig. 3. Samples P01, P02 and P03 (dried powders) were measured in both Bragg-Brentano geometry and parallel beam technique with the angles of incidence of 1 - 3 ° by using of XRD-FPM and X'Pert MRD Pro diffractometers. Sample G01 (thin layer of TiO_2 nanotubes on support glass) was measured only by the latter method. The results obtained by the parallel beam technique only are shown on Fig. 3. Technical powder consists of pure anatase phase while the nanopowder was a mixture of anatase and rutile. Three quite narrow peaks obtained from sample G01 does not correspond strictly to any of the known TiO_2 phases. Nanotubes from powder (P03) also give rather different diffraction pattern (Fig. 4d). Similar pattern was found by the authors of [2]. They reported trititanate $H_2Ti_3O_7$ nanotubes. In our case the correspondence to this phase is not so good. Better agreement could be found for another phase - hydrogen titanium oxide hydrate $H_2Ti_2O_5 \cdot H_2O$. The correspondence of intensities is not very good but specific features of the diffraction by nanotubes have not been incorporated into calculation yet. The comparison on Fig. 4 is only performed with the PDF patterns [4].

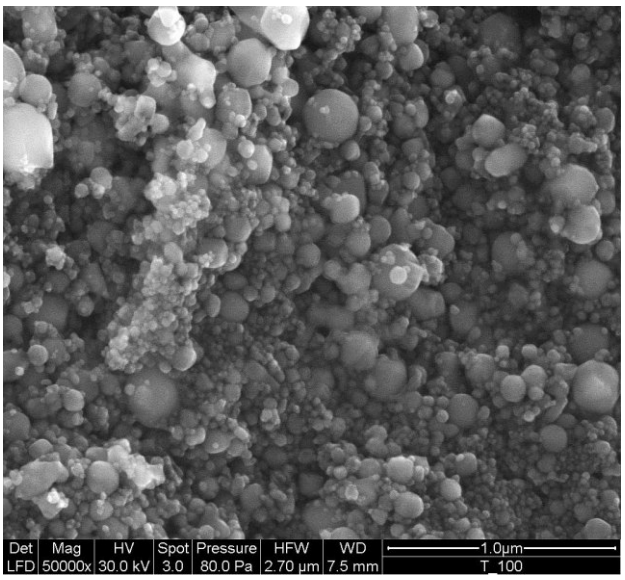

Fig . 1. SEM micrograph of the original TiO_2 nanopowder

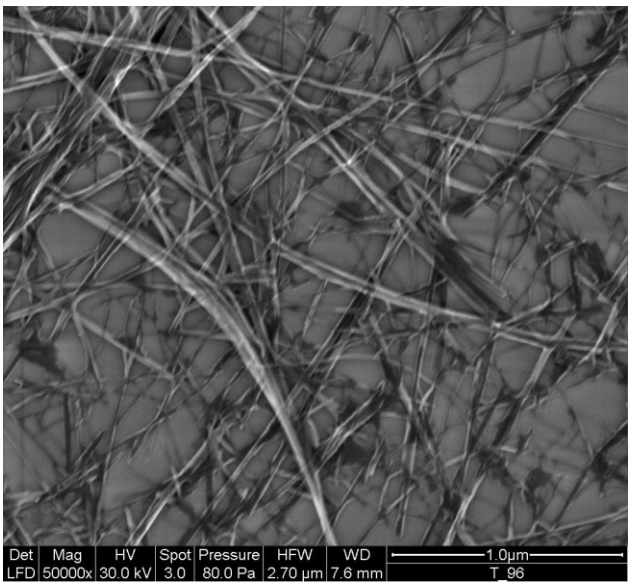

Fig. 2. SEM micrograph of TiO_2 nanotubes; the first preparation procedure.

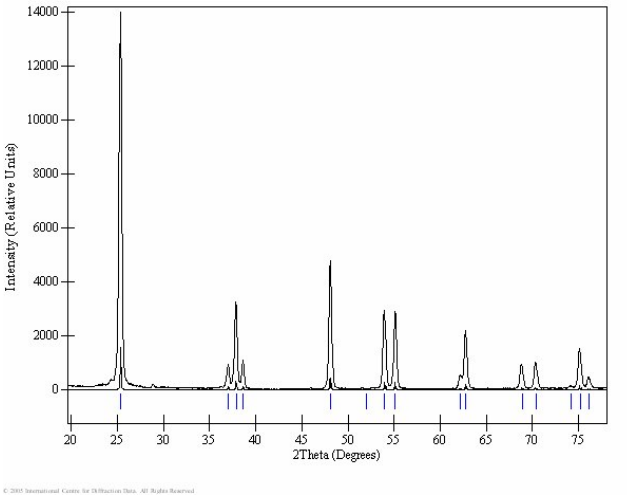

(a) Sample P01: commercial technical powder; pure anatase.

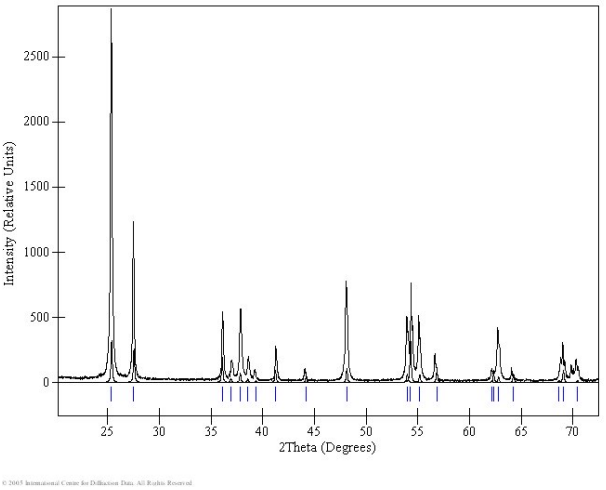

(b) Sample P02: commercial nanopowder; mixture of anatase and rutile.

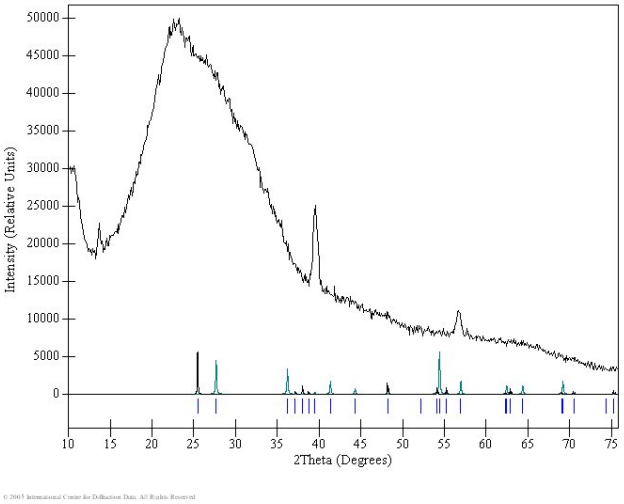

(c) Sample G01: nanotubes from solution.

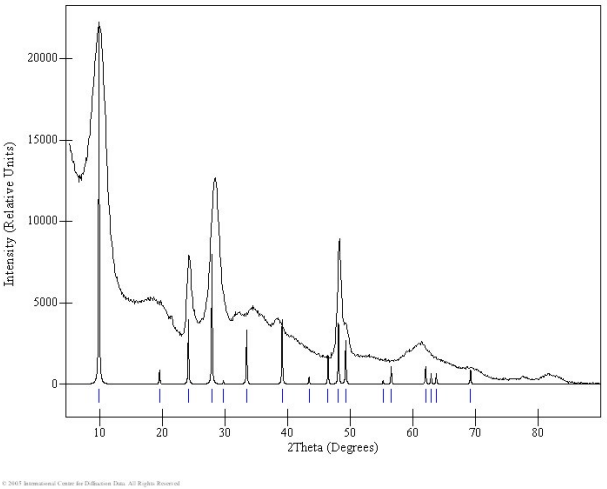

(d) Sample P03: nanotubes from powder; the diffraction pattern is similar to $H_2Ti_2O_5.H_2O$, differing from rutile, anatase and brookite.

Fig. 3. Diffraction patterns of TiO_2 samples obtained in parallel beam geometry.

Acknowledgements*: MŠ is indebted for financial support trough grant 203/04/0688 awarded by the Grant Agency of the Czech Republic and for the participation in the EU Network of Excellence „Nanostructured Multifunctional Polymer Based Materials and Nanocomposites"(NANOFUN -POLY). RK acknowledges the support through research program MSM 0021620834 financed by the Ministry of Education of the Czech Republic.*

1. T. Kasuga, M. Hiramatsu, A. Hoson, T. Sekino, K. Niihara, *Adv. Mater.*, **11**, (1999), No.15.
2. Q. Chen, W. Zhou, G. Du, L. Peng, *Adv. Mater.* ,**14**, (2002), No.17.
3. Y. F. Chen, C. Y. Lee, M.Y. Yeng, H. T. Chiu, *Materials Chemistry and Physics*, **81**, (2003), 39-43.
4. PDF4+. Powder Diffraction File. ICDD. www.icdd.com.

P17

WHOLE POWDER PATTERN ANALYSIS OF THIN TiO_2 LAYERS

Z. Matěj, L. Nichtová and R. Kužel

Department of Electronic Structures, Faculty of Mathematics and Physics, Charles University, Ke Karlovu 5, 121 16 Praha 2, Czech Republic, matej@karlov.mff.cuni.cz

TiO_2 nanopowders appear many special properties. In numerous practical applications only thin surface region is significant for desired product functionality and hence it is not surprising that also thin TiO_2 films are a matter of interest. Investigated TiO_2 layers were prepared by magnetron sputtering (ZČU Plzeň) and they consist from an amorphous component and two most common TiO_2 crystalline phases: anatese and rutile. It is suspected that there is a surface anatase rich film on a rutile rich substrate layer. This hypothesis should be clarified by detailed X-ray diffraction study.

A computer program for whole powder patter fitting of our samples was developed. It is based on a crystallographic computing library ObjCryst++ (a program Fox) [1] which is in the program used for structure factors and whole powder pattern calculations. Library fitting algorithms are employed there as well. Intensity corrections for the parallel beam geometry accounting for absorption in the layered structure of the samples, simple texture description, background correction and microstructural models [2,3] for profile shape evaluation were mixed in the program to simulate measured data.

1. V. Favre-Nicolin, R. Černý, *J. Appl. Cryst.*, **35** (2002) 734-743.
2. P. Scardi, M. Leoni, *Acta Cryst. A*, **58** (2002) 190-200.
3. G. Ribárik , T. Ungár, J. Gubicza, *J. Appl. Crys.*, **34** (2001) 669-676.

Acknowledgements.

We would like to express our thanks to V. Fafre-Nicolin and teams of T. Ungár and P. Scardi for opportunity of using and testing their computer programs. This work is a part of the research plan MSM 0021620834 that is financed by the Ministry of Education of the Czech Republic.

P18

GROWTH OF NANOCRYSTALLINE MAGNETRON SPUTTERED TiO_2 THIN FILMS STUDIED BY X-RAY SCATTERING

R. Kužel[1], L. Nichtová[1], Z. Matěj, D. Heřman[2], J. Musil[2]

[1]Faculty of Mathematics and Physics, Charles University in Prague, Czech Republic;
[2]Faculty of Applied Sciences, University of West Bohemia in Pilsen, Czech Republic

Titanium dioxide films are widely used because of their excellent properties as chemical stability, mechanical hardness and optical transmittance with high refractive index. The photocatalytic activity of TiO_2 can result in the decomposition of organic compounds on the TiO_2 surface or the reduction of the contact angle between water and the TiO_2 surface under ultraviolet irradiation. The films can be prepared by several techniques but the magnetron deposition is favourable from the point of view of mechanical durability required for practical applications. Depending on the deposition conditions, the films can be prepared as amorphous or nanocrystalline.

In the present work, a complex XRD study was performed on the films sputtered by dual magnetron on the glass and single-crystal silicon substrates. A set of nanocrystalline films with different thickness in the interval of 0.1 m to 2 m was investigated after the deposition. The measurement was performed on Philips X'Pert MRD in parallel beam setup, 2 scans with very low angles of incidence with collimators and Goebel mirror in the primary beam. X-ray reflectivity curves were measured too. The curves dropped rapidly for all the samples except the thinnest one (0.1 m). In addition, contact angles of water drops on the film surface were measured after different periods of films irradiation by UV light.

The films deposited on glass subrate shown similar behaviour to the ones on Si substrate in many cases but there are also significant differences. The films on silicon show usually more pronounced texture. The most important differences were found in the phase composition for the thinnest samples, though. The thinnest film (0.1 m) on glass substrate was amorphous while for the same film on silicon clear broad peaks of rutile were detected. Similarly, for the film with the thickness of 0.2 m (Fig. 1a) for which small rutile peaks can also be seen on glass substrate. For none of these thin films any significant decrease of the drop contact angle after UV irradiation was found even though there are visible differences in their surface roughness. The angles remained on high values (65 - 75°). For the films thicker than 0.5 m, anatase is clearly dominating phase (Fig. 1b, 1c) and for the 2 m thick film only pure anatase was detected.

A set of measurements with different angles of incidence 0.5 – 5° and consequently also different penetration

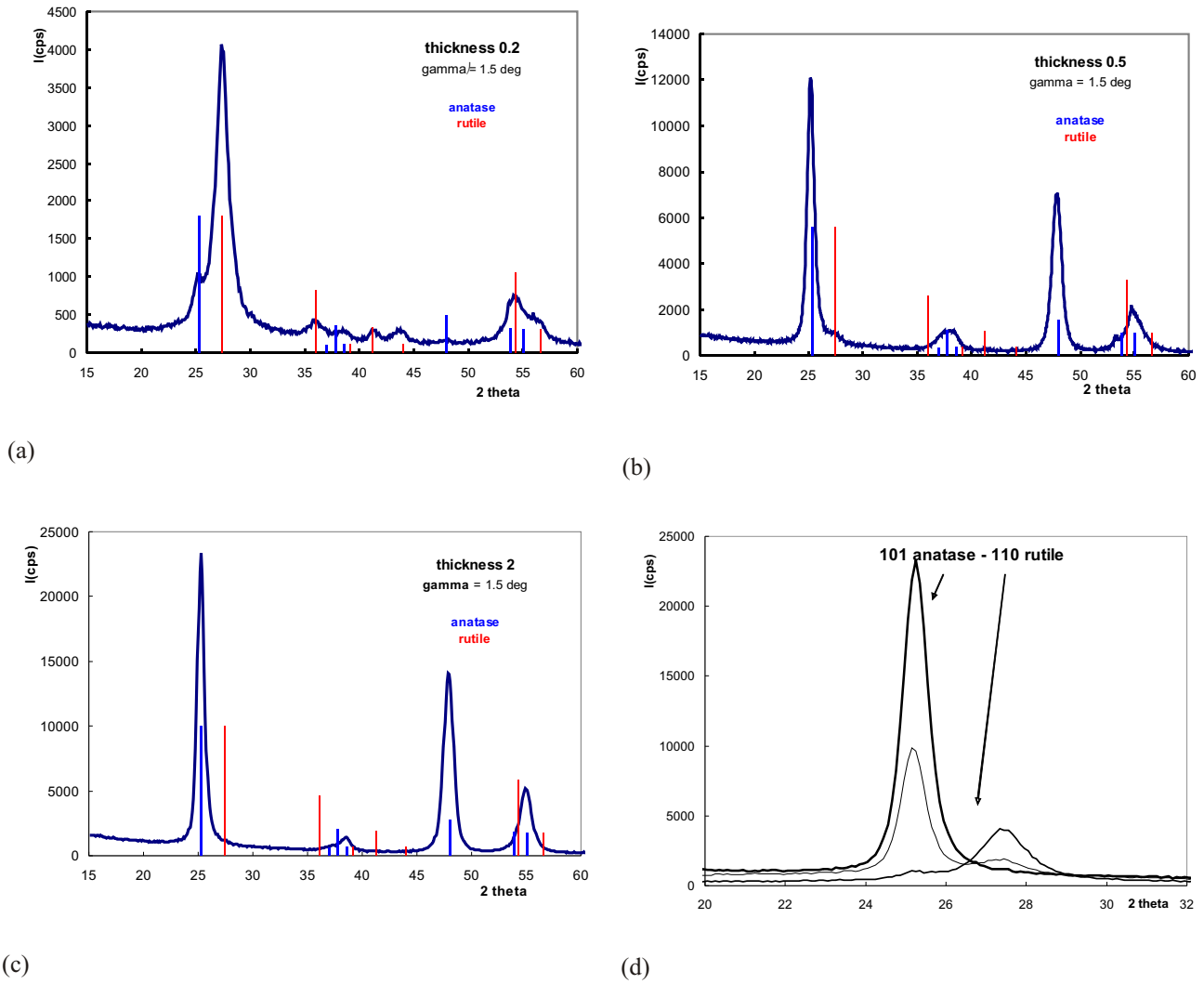

Fig. 1. Diffraction patterns of TiO_2 films with different thickness – a) 0.1 m, b) 0.5 m, c) 2 m. The patterns were obtained in parallel beam optics and 2 scan and fixed angle of incidence – 1.5 . In Fig. 1d) – patterns from the sample with the thickness 0.9 m, obtained at different angles of incidence – lower thick line - 0.5 , middle thin line - 1.0 , upper thick line - 1.5 . Thick bars indicate theoretical peak positions for anatase, thin bars correspond to the peaks of rutile.

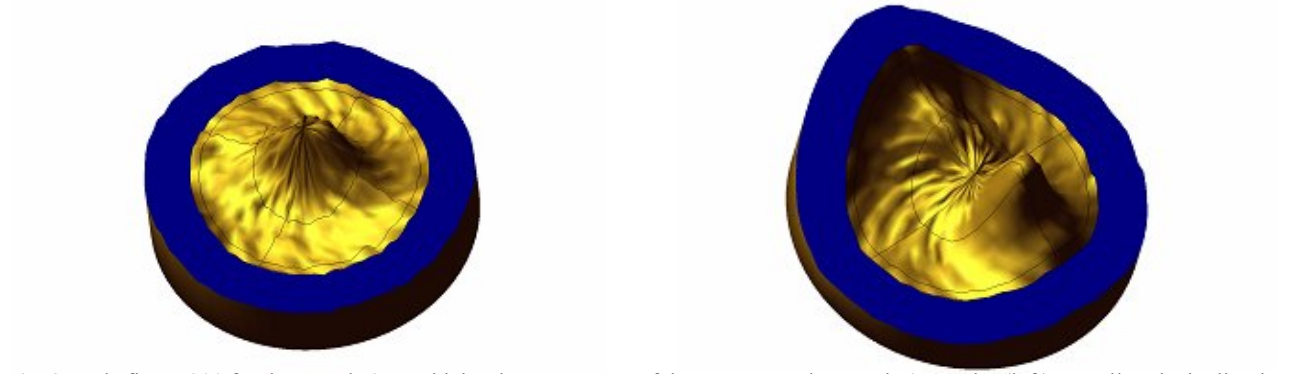

Fig. 2. Pole figure 200 for the sample 2 m thick. The asymmetry of the texture can be seen in 2.5D plot (left) as well as the inclination of the texture on Si substrate.

depths (the penetration depth for the smallest angle of incidence is below 200 nm) clearly show that rutile grows on the interface with both Si and glass substrates in all cases but its growth is supressed for thicker films by anatase which is mainly on the top (Fig. 1d). Since for all the thicker films the angles of water drops were drastically reduced after UV irradiation (5 hrs irradiation, down to 10 – 20°), it seems that only anatase is favourable in this case for hydrophilicity and by contrast rutile makes films hydrophobic. Differences between both substrates were also

found. The films on silicon have better hydrophilicity than corresponding films on glass. From the structural point of view, the former have slightly better crystallinity and more pronounced texture.

Because of very broad peaks, the detailed measurement of residual stresses could be performed on the Eulerian cradle by the $\sin^2$ method only for two different peaks of anatase phase (101, 200). The dependences were strongly curved but with the absence of splitting for negative and positive inclination angle which could indicate triple-axis stresses. The curvature can be ascribed to the texture. The plots are also very different for both peaks. For the peaks 101 and 200 the pole figures have also been measured and shown the presence of (100) texture. The texture was not completely fiber and for samples on Si it was significantly inclined with respect to the surface (Fig. 2). The asymmetry of the texture can be well understood, if we take into account that the deposition was made by dual magnetron.

This work is supported by the Grant Agency of the Czech Republic, no. 106/06/0327.

P19

POWDER X-RAY DIFFRACTION FROM MULTILAYER IN A GRAZING-INCIDENCE NON-COPLANAR GEOMETRY

L. Horák and V. Holý

Department of Electronic Structures, Charles University, Prague, Czech Republic
e-mail: Lukas.horak@napismi.cz

X-ray powder diffraction in a non-coplanar grazing-incidence geometry makes it possible to determine lateral grain sizes and strains in polycrystalline multilayers. The depth profile of these quantities can be also determined using a standing X-ray wave generated in the multilayer by the interference of the primary and specularly reflected beams [1].

The grains of a polycrystalline layer are irradiated by the standing wave so that the intensity of the diffracted beam is modulated by the standing wave pattern. Similarly, the radiation diffracted by the polycrystalline grains reflects specularly from the interfaces in the multilayer and another standing wave pattern results, which affects the diffracted intensity as well.

Changing the incidence angle, we move the positions of the antinodes of the standing-wave pattern so that this method makes it possible to study the vertical profile of the parameters of the polycrystalline layer because total intensity are mostly given by the contribution of grains near antinodes.

We use this concept for the investigation of polycrystalline single layers and periodic multilayers. For both sample types, we have measured the distribution in the diffracted intensity in the angular ($_i$,2) plane; the measurements have been carried out using a conventional laboratory diffractometer allowing for a non-coplanar scattering geometry equipped with a polycapillary optics and a secondary flat monochromator, intensity was integrated over $_f$ in a range given by detector's window. We have measured these samples using a synchrotron radiation and in this case we have used several wavelengths (for example near absorption edge) and position sensitive detector so the intensity has been measured in $_f$ axis too.

The measured intensity distributions we have compared with simulations based on the distorted-wave Born approximation and kinematical scattering theory [1,2] to determine the grain sizes and their vertical profile. Parameters of the multilayers such as thickness and relative density we have obtained from X-ray reflectivity.

Whole these processes in sample we describe using distorted-wave Born approximation, the goal is to solve wave equation and we consider scattering potential divided to two potentials, undisturbed system without crystal lattice, this we are able to solve exactly using dynamic theory, this potential leads to wave field in sample [2]. The second potential is given by crystal lattice and it is a disturbance of the first potential. Assuming that grains are much smaller than extinction length and they diffract kinematically, we solve disturbance using kinematical theory and wave field given by undisturbed solution [1].

This method is suitable for probing multilayers and even single thin layer on a substrate. The greatest advantage is sensitivity to depth and ability to get information from thin layers, on the other hand there are strict requirements to roughness and lateral homogeneity, the sample has to be suitable for X-ray reflectivity measurement.

1. P. F. Fewster, N. L. Andrew, V. Holý, and K. Barmak, *Phys. Rev. B* **72**, 174105 (2005).
2. U. Pietsch, V. Holý, and T. Baumbach, *High Resolution X-Ray Scattering - From Thin Films to Lateral Nanostructures* (Springer, 2004).

P20

X-RAY STANDING-WAVE EFFECTS IN GRAZING-INCIDENCE X-RAY DIFFRACTION FROM POLYCRYSTALLINE MULTILAYERS

J. Krčmář[1] and V. Holý[2]

[1]*Institute of Condensed Matter Physics, Masaryk University Brno, Czech Republic,*
[2]*Department of Electronic Structures, Charles University Prague, Czech Republic*

Grazing-incidence geometry is frequently used in powder x-ray diffraction from thin polycrystalline layers, since it allows suppressing the diffraction from substrates. If this geometry is used for a polycrystalline periodic multilayer, the diffracted intensity is modulated by a standing wave created by the interference of the radiation transmitted through the multilayer stack with the wavefields specularly reflected from the superlattice interfaces. Similarly, the radiation being diffracted from the polycrystalline structures is reflected specularly from the interfaces and a standing-wave interference pattern results as well.

The standing-wave effects in diffraction from polycrystals have been analyzed theoretically in our previous work [1], this presentation demonstrates a series of experimental measurements obtained from Ni/C periodic multilayers. The measurements have been carried out at ESRF using x-ray energies far away and close to the NiK absorption edge, so that anomalous scattering effects were present. The experimental data have been modeled using a theoretical approach based on the distorted-wave Born approximation and a good fit to the theory was achieved.

The experimental data obtained demonstrate that the method can be used for the investigation of the polycrystalline multilayers, especially for studying the profiles of the grain sizes and strains across the multilayer stack.

The work has been supported by the Ministry of Education of the Czech Republic (Research project MSM002162 2410).

1. P. F. Fewster, N. L. Andrew, V. Holý, and K. Barmak, *Phys, Rev.* **B72** (2005) 174105.

P21

IN-SITU INVESTIGATIONS OF Si AND Ge INTERDIFFUSION IN Si CASCADE STRUCTURES

M. Meduňa[1], J. Novák[1], V. Holý[1], C.V. Falub[3], G. Bauer[2], and D. Grützmacher[3]

[1]*Institute of Condensed Matter Physics, Masaryk University, Kotlářská 2, Brno, Czech Republic*
[2]*Institute of Semiconductor Physics, J. Kepler University, Altenbergerstrasse 69, Linz, Austria*
[3]*Laboratory for Micro- and Nanotechnology, PSI, Villigen-PSI, Switzerland*

The importance of knowledge of diffusion properties of Si and Ge is crucial for production of SiGe based cascade emitters. Electroluminescence has been observed from specially designed Si/SiGe quantum cascade structures [1] and the implementation of quantum cascade laser in SiGe technology is still in demand. Nevertheless heating due to thermal losses during operation of such devices is a significant factor and the knowledge of the temperature stability of cascade structures and the diffusion processes of Ge and Si in SiGe are very important.

The diffusion properties of Ge in either Si or in $Si_{1-x}Ge_x$ alloys are still not well understood. Their determination is complicated by the strong non-linear dependence of interdiffusion coefficient $D = D_0(X_{Ge})\exp[-E_A(X_{Ge})/kT]$ on Ge content X_{Ge} in $Si_{1-x}Ge_x$ [2]. In recent publications [3] only activation energies E_A and diffusion prefactors D_0 for X_{Ge} up to Ge contents of 50 % were reported with comparatively large error bars. To our knowledge the parameters E_A and D_0 for $Si_{1-x}Ge_x$ in the range of X_{Ge} from 0.5 to 1 are not well reported, but they are necessary for the numerical modeling of non-linear diffusion processes of Si and Ge in $Si_{(1-x)}Ge_x$ cascade structures with Ge contents up to 80%. Since the typical cascade structures are very complicated and the evaluation and analysis of its measured data are quite difficult, the most suitable for X-ray measurements are simple MQW structrures.

In our case we have studied series of strain symmetrized MQW structures grown on $Si_{0.25}Ge_{0.25}$ and $Si_{0.5}Ge_{0.5}$ pseudosubstrates with thicknesses and periods similar to usual cascade structures. The Ge content in these structures was 30 % and 80 % with multilayer periods in the range from 6 to 13 nm. X-ray reflectivity (XRR) and diffraction (XRD) reciprocal space maps for all structures have been recorded at room temperature and during several in-situ isothermal annealing processes for temperatures ranging from 550 °C up to 824 °C. The annealing was performed under high vacuum using a Be dome chamber at ROBL beamline at ESRF [4].

The obtained measurements were compared with simulations of diffraction curves for MQW structures using the evolution of Ge content profile according to nonlinear diffusion equation.

The Ge content profile obtained from diffusion equation was used for simulating the XRR or XRD spectra.

Since the interdiffusion coefficient depends strongly on Ge content, the interpretation of the data is still quite difficult.

1. L. Diehl, S. Mentese, E. Müller, D. Grützmacher, H. Sigg, T. Fromherz, J. Faist, U. Gennser, Y. Campidelli, O. Kermarrec, D. Bensahel, *Physica E*, **16** (2003) 315.
2. N. R. Zangenberg, J. L. Hansen, J. Fage-Pedersen, and A. N. Larsen, *Phys. Rev. Lett.*, **87** (2001) 125901.
3. D. B. Aubertine, M. A. Mander, N. Ozguven, A. F. Marshall, P. C. McIntyre, J. O. Chu and P. M. Mooney, *J. Appl. Phys*., **92** (2002) 5027.
4. M. Meduňa, J. Novák, C.V. Falub, G. Chen, G. Bauer, S. Tsujino, D. Grützmacher, E. Müller, Y. Campidelli, O. Kermarrec, D. Bensahel, N. Schell, *J. Phys. D: Appl. Phys*., **38** (2005) A121.

P22

X-RAY DIFFUSE SCATTERING FROM OXYGEN-BASED DEFECTS IN CZOCHRALSKI SILICON

P. Klang[1] , V. Holý[1,2]

[1]Institute of Condensed Matter Physics, Masaryk University, Brno, Czech Republic
[2]Faculty of Mathematics and Physics, Charles University, Prague, Czech Republic
klang@physics.muni.cz

Silicon single crystals grown by the Czochralski method contain oxygen impurities in the concentration of about 10^{18} cm^{-3}. Annealing at high temperatures leads to the formation of amorphous SiO_2 precipitates, which create traps for fast diffusing metallic contaminants [1]. The understanding of the formation and growth of these oxygen-based defects plays an important role in fabrication of integrated circuits.

Czochralski grown silicon wafers (111) were studied using triple-axis high resolution X-ray diffraction. We have measured reciprocal space maps of intensity distribution from the scattering on defects in silicon wafers after annealing processes (see Fig. 1(a)). The samples were annealed at 1000 °C for different periods in order to study the growth of oxygen-based defects. In the radial cross-section of the measured map we can find different types of scattering - Huang scattering (HS) for small q, Stokes-Wilson scattering (SWS) for middle q and thermal diffuse scattering (TDS) for large q (see Fig. 1(b)).

We have also modelled the reciprocal space maps of intensity distribution using the Krivoglaz theory [2] and a continuum model of the defect deformation field. From the comparison, we have determined the size, symmetry and concentration of the defects, as well as the deformation field in their neighbourhood.

1. C. Newman, *J.Phys.: Condens. Matter* **12** (2000) R335.
2. M. A. Krivoglaz in *Diffraction of X-rays and Neutron in Nonideal Crystals* (Springer, Berlin), 1996.

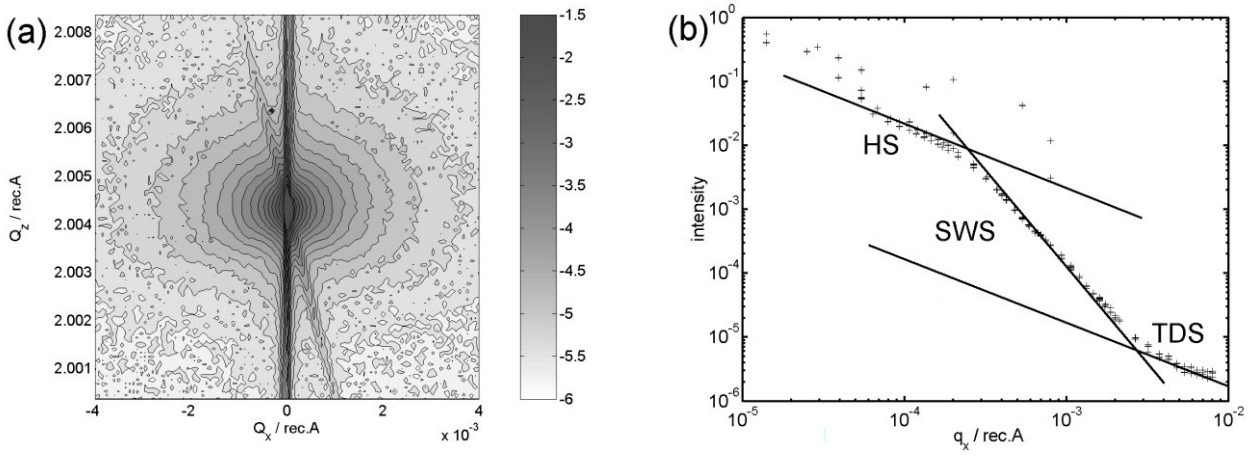

Fig. 1. (a) Measured symmetrical reciprocal space map (111) of the sample annealed at 1000 °C for a period of 16 h, (b) radial cross-section of this map along the q_x direction with the different types of the scattering.

P23

SPATIAL m-RESOLVED STRUCTURE CHARACTERIZATION OF SEMICONDUCTOR WAFERS AND LATERAL OVERGROWTH STRUCTURES BY SYNCHROTRON RADIATION ROCKING CURVE IMAGING

P. Mikulík[1], D. Lübbert[2,3], L. Helfen[2], P. Pernot[2], S. Keller[4], T. Baumbach[2]

[1]Institute of Condensed Matter Physics, Masaryk University, Brno, Czech Republic
[2]ANKA / Institute for Synchrotron Radiation, Forschungszentrum Karlsruhe, Germany
[3]Humboldt-Universität, Berlin, Germany
[4]University of California at Santa Barbara, CA, USA
mikulik@physics.muni.cz

We present recent advances on local lattice and structure quality control of semiconductor wafers and overgrown structures with spatial resolution down to one micrometer over an extended sample area. We employ synchrotron radiation diffraction rocking curve imaging (RCI) technique, which combines digital X-ray topography and conventional Bragg-diffraction rocking curve recording. Application of this method has been pushed from qualitative wafer structure characterization towards quantitative mapping of local crystalline misorientations and dislocation density and towards one-micrometer spatial resolution to study crystalline morphology of overgrown patterned structures [1, 2, 3].

Growth of compound materials in ingots, like SiC, GaAs, GaN, InP, leads to inherited imperfections. Regions of specific misoriented macrodefects and dislocation regions in ingots can be qualitatively mapped by RCI [1], see figure 1. Epitaxial lateral overgrowth (ELO) is an innovative crystal growth technique expected to achieve a better crystal quality. The overgrown layer shows significantly lower density of threading dislocations than in the wetting layer. With micrometer-resolved 2D detector, the RCI allows to monitor the lattice quality and lattice tilts in individual periods of the structure [2], see figure 2. Significant information can be obtained from individual sample areas as small as 2 micrometers in all three spatial dimensions, and to check the findings of double-crystal diffraction rocking curve measurements.

1. P. Mikulík, D. Lübbert, D. Korytár, P. Pernot, and T. Baumbach, *J. Phys. D: Appl. Phys.*, **36** (2003) A74.
2. D. Lübbert, T. Baumbach, P. Mikulík, P. Pernot, L. Helfen, R. Köhler, T.M. Katona, S. Keller, S.P. DenBaars, *J. Phys. D: Appl. Phys.*, **38** (2005) A50.
3. P. Mikulík, D. Lübbert, P. Pernot, L. Helfen, T. Baumbach, *Appl. Surf. Sci.*, (2006), in print.

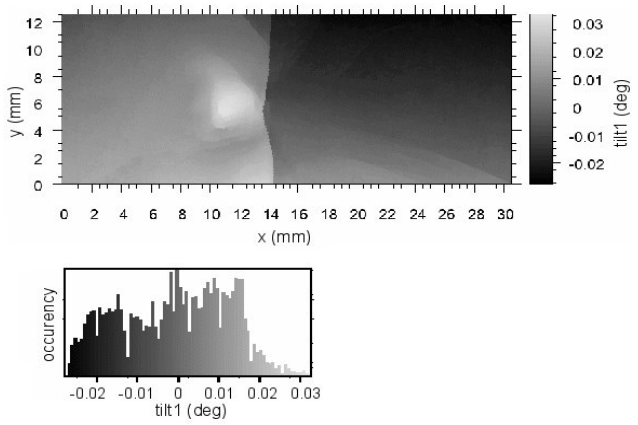

Fig. 1. A lattice tilt component distribution in a specific area on a GaAs wafer [3].

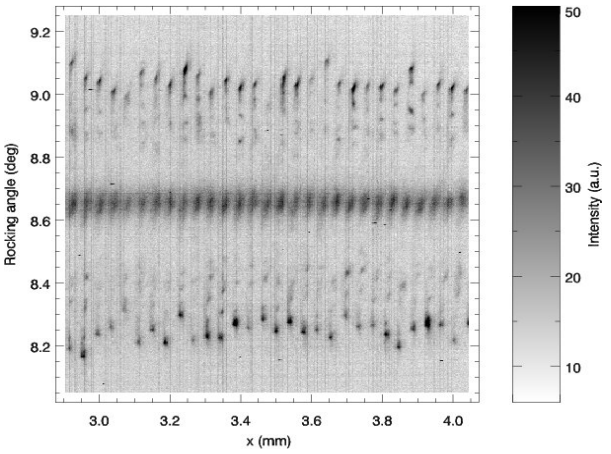

Fig. 2. Angular separation of the GaN ELO column vs. wings (centre vs. top and bottom spots) [3].

P24

CAN WE DISTINGUISH BETWEEN MISFIT AND THREADING DISLOCATIONS USING X-RAY DIFFUSE SCATTERING EXPERIMENT? THE CASE OF PbTe THIN LAYERS

S. Daniš and V. Holý

Department of Electronic Structures, Faculty of Mathematics and Physics, Charles University Prague, Ke Karlovu 5, 121 16 Prague 2, Czech Republic
e-mail:danis@mag.mff.cuni.cz

X-ray diffuse scattering is a commonly used tool for determination of real structure in monocrystals, powders and low dimensional systems. If there is only one type of defect in the sample (clusters of atoms in ion-bombarded silicon, for example), the situation is quite simple. The size and concentration of the defect can be determined by reciprocal space maps. However, in the case of relaxed heteroepitaxial thin layers, we have to deal with misfit and threading dislocations.

Intensity of diffuse X-ray scattering is given by displacement of atoms caused by the defect(s). The displacement fields are simulated within isotropic theory of elasticity. The total intensity is calculated within kinematical theory of x-ray scattering,

$$I(q) \quad A \int_V d^3\mathbf{r} \int_V d^3\mathbf{r}' \exp\ (i\mathbf{q}\ (\mathbf{r} \quad \mathbf{r}'))\exp(\ T_h(\mathbf{r},\mathbf{r}'))$$

where A is, among others, a constant containing square of the sample polarizability, V is the layer volume, $\mathbf{q} = \mathbf{Q}\text{-}\mathbf{h}$ is the coordinate in reciprocal space relative to the reciprocal lattice point $\mathbf{h}$, $\mathbf{Q} = \mathbf{K}_f - \mathbf{K}_i$ is the scattering vector. $T_\mathbf{h}(\mathbf{r},\mathbf{r}')$ is correlation function of defects defined as a sum of contribution from threading and misfit dislocations,

$$T_h(\mathbf{r},\mathbf{r}') \quad T_{h,threading} \quad T_{h,misfit}$$

Diffuse X-ray scattering from epitaxial PbTe layer on Si(111) is analyzed both theoretically and experimentally. Reciprocal space maps (RSM) and X-ray diffraction profiles are measured and simulated for symmetrical and asymmetrical diffractions. The intensity distribution of diffusively scattered radiation is simulated within statistical theory of X-ray scattering [1, 2]. Both types of expected defects -misfit and threading dislocations – will be discussed.

1. M. A. Krivoglaz, *X-Ray and Neutron Diffraction in Nonideal Crystals*, (Springer Berlin 1996).
2. V. M. Kaganer, R. Koehler, M. Schmidbauer, R. Opitz, and B. Jenichen, *Phys. Rev. B* **55**, 1793 (1997).

P25

GRADIENTS OF REAL STRUCTURE IN SURFACE LAYERS

J. Drahokoupil[1,2,*], M. Čerňanský[1], N. Ganev[2], K. Kolařík[2], Z. Pala[2]

[1]*Institute of Physics, Academy of Sciences of the Czech Republic, Na Slovance 2, 182 21 Praha 8, Czech Republic*
[2]*Faculty of Nuclear Sciences and Physical Engineering, Trojanova 13, 120 00 Praha 2, Czech Republic*
jandrahokoupil@seznam.cz

Gradients of parameters of the real structure after surface machining have been studied by X-ray diffraction in steels. A surface is much more deformed than an inside, which may be without any modification. The parameters of the real structure, e.g., macroscopic residual stress, microstrain, and particle size have been studied. It is very useful to make measurements under various conditions (i.e., various angles more diffraction lines; several types of radiations). For describing radiation penetration depth into matter the term "effective depth of penetration" can be used. It can be computed, in case of -diffractometer, as follows

$$T^{ef} \quad \frac{1}{f(\ ,\ )} \quad \frac{\sin^2 \quad \sin^2}{\sin \ ^2 \cos} \qquad (1)$$

where ( ) linear absorption coefficient, $f(\ )$ – function dependent on type of scan, - Bragg angle and - tilt angle.

The mean value of some parameters which changes with depth is given by

$$\bar{x} \quad \frac{\int_0^h x(T)\exp(\quad Tf(\ ,\ ))dT}{\int_0^h \exp(\quad Tf(\ ,\ ))dT} \qquad (2)$$

where $x\ (T) = x^0 + x^1 T + x^2 T^2 + \ldots$ (polynomial dependencies supposed); x – represents particle size D, microstrain e, or stress $_{ij}$, and in some special cases x may also represent lattice parameter; h – thickness of specimen and T – variable of depth.

The general least-squares analysis was used to obtain the parameters of the real structure. To study the residual

macroscopic stress, the following general equation can be written as [1]

$$\overline{}_{hkl} \quad \frac{1}{2} s_1^{hkl} [\overline{}_{11} \cos^2 \quad \overline{}_{12} \sin 2 \quad \overline{}_{22} \cos^2 \quad) \sin^2$$
$$\overline{}_{33} \cos^2 \quad (\overline{}_{13} \cos \quad \overline{}_{23} \sin \quad) \sin 2 \quad]$$
$$s_1^{hkl} (\overline{}_{11} \quad \overline{}_{22} \quad \overline{}_{33}) \qquad (3)$$

To determinate the particle size and the microstrain, the integral breadth was separated exactly as it is used in the single line Voigt function method [2]. Then the particle size and the microstrain may be obtained by:

$$D \quad \frac{K}{{}_c \cos} \,, \; e \quad \frac{{}_G}{4 \tan} \qquad (4, 5)$$

Where ${}_c$ and ${}_g$ are the Cauchy and Gaussin components of the integral breadth.

1. U. Welzel, J. Ligot, P. Lamparter, A. C. Vermeulen and E. J. Mittemeijer, *J. Appl. Cryst*., **3** (2005) 1.
2. Th. H. de Keijser, J. I. Langford, E. J. Mittemeijer and A. B. P. Vogels, *J. Appl. Cryst*., **15** (1982) 308.

Acknowledgements.
The research was supported by the Project ą 101/05/2523 of the GA of the Czech Republic and by the Nat. Res. Projects AV0Z10100520, AV0Z10100522 of the Czech Republic.

P26

STUDY OF RESIDUAL STRESS OF A HIGH – ALLOY TOOL STEELS AFTER ELECTRO DISCHARGE MACHINING

K. Kolařík and N. Ganev

Department of Solid State Engineering, Faculty of Nuclear Sciences and Physical Engineering, Czech Technical University in Prague, Trojanova 13, 120 00 Prague 2, Czech Republic

The objective of this contribution is investigation of residual stress state and distribution of microhardnes in surface layers of samples subjected to progressive unconventional technology electro discharge machining (EDM). Experimental samples were machined using graphite and electrolytic copper electrodes in common technological processes of finishing and stocking. Results of X - ray diffraction technique comply with the assumption that the layers machined by EDM exhibit isotropic biaxial residual stress state.

Introduction

The long-term experiences with applications of EDM and investigations of surface layers show that specific changes occur; their usual distribution is demonstrated in Fig. 1.

The intensity of removal of material during EDM is proportion to the energy of electrical discharge which is supplied by the generator of the machine tool. Except the energetic parameters (e. g. voltage, current, time of discharge) a large array of other factors determine the surface state and therefore its quality. Physical properties of the electrodes, which consist of the tool and the work-piece, belong among the most decisive parameters and hence the choice of polarity of discharge generator plays a crucial role. The aim of this contribution is to focus on the relation between the final state of the surface and the properties of electrodes, because the construction of generator and the recommendations of producers of tools vary.

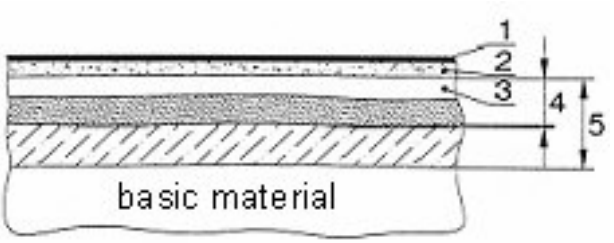

Fig. 1. Surface layer of steel affected by EDM [1].
1- microlayer of chemical compounds which originated during diffusion of dielectric, 2 – layer containing the material of tool electrode, 3 – the so called "white layer", strongly armorized resolidated melt, fine martensite-like structure, hardness 60 HRC, thickness from 0.04 mm to 0.3 mm depending on the energy of pulses, 4 – heat affected zone (hardened and tempered basic material of work-piece), 5 – plastic deformation zone induced by surges.

Samples under investigation

The experimental samples of dimensions 30 30 7 mm^3 were made from high-ally tool chrome steel ČSN 19436 (C 1.8 – 2.05 %, Mn 0.20 – 0.45 %, Si 0.20 – 0.45 %, P 0.03 %, S 0.035 %, Cr 11.0 – 12.5%, Ni 0.50 %). One half of the samples was left in basic state, the other was hardened according to the standard ČSN 41 436 [2] onto secondary hardness 58 - 60 HRC (heating in a vacuum furnace at austenitic temperature 1070 °C, hardening in oil bath and double tempering at 490 °C).